Available online at www.sciencedirect.com
ScienceDirect
Journal of Hazardous Materials 149 (2007) 742–746
Journal of Hazardous Materials
www.elsevier.com/locate/jhazmat

Short communication

Catalytic combustion of toluene over platinum supported on Ce–Zr–O solid solution modified by Y and Mn

Zhi Min Liu [a], Jian Li Wang [a], Jun Bo Zhong [a,b], Yao Qiang Chen [a], Sheng Hui Yan [a], Mao Chu Gong [a,*]

[a] College of Chemistry, Sichuan University, Chengdu 610064, Sichuan, PR China
[b] Department of Chemistry, Sichuan University of Science and Engineering, Zigong, 643000, Sichuan, PR China

Received 28 January 2007; received in revised form 13 August 2007; accepted 13 August 2007
Available online 19 August 2007

Abstract

A series of CeO_2–ZrO_2 mixed oxides were prepared using coprecipitation method and characterized by BET, oxygen storage capacity (OSC), X-ray diffraction (XRD) and H_2-temperature-programmed reduction (H_2-TPR). The catalytic activities toward toluene combustion were investigated in a micro-reactor. The results demonstrate that the catalytic activity of Pt/γ-Al_2O_3/$Ce_{0.50}Zr_{0.50}O_2$ monolithic catalyst can be greatly improved by doping metal into $Ce_{0.50}Zr_{0.50}O_2$. When doping Y and Mn into $Ce_{0.50}Zr_{0.50}O_2$ simultaneously, the catalyst Pt/γ-Al_2O_3/$Ce_{0.40}Zr_{0.40}Y_{0.10}Mn_{0.10}O_X$ shows the highest activity. The T_{10} (the temperature of 10% toluene conversion) and the complete conversion temperature (the temperature of 90% toluene conversion) of toluene are 443 and 489 K, respectively. Gas hourly space velocity (GHSV) results show that the prepared catalyst can be applied in a wide range of GHSV (from 12,000 to 20,000 h^{-1}). The catalyst prepared shows great potential for practical application.

Keywords: $Ce_{0.50}Zr_{0.50}O_2$; Catalytic combustion; Toluene; Doping; Gas hourly space velocity

1. Introduction

Volatile organic compounds (VOCs), especially aromatic hydrocarbons, are typical pollutants emitted from numerous urban and industrial sources. Their extensive use leads to water and air pollution. Many of the VOCs in common use are toxic and some are considered to be carcinogenic, mutagenic, or teratogenic [1]. The most significant problem related to the emission of VOCs is centered on the potential production of photochemical oxidants, for example, ozone and peroxyacetyl nitrate [2]. Emissions of VOCs also contribute to localized pollution problems of toxicity and odor. Many VOCs are implicated in the depletion of the stratospheric ozone layer and may contribute to global warming [3].

As a result of all these problems, VOCs have drawn considerable attention in the last 30 years. With this respect, stringent international regulations are applied for different sources of such compounds [4]. Conventional methods for treating VOCs from gas streams, such as absorption, adsorption, condensation and thermal incineration, all have inherent limitations and none is definitely cost-effective [5]. Among the technologies developed for the treatment of VOCs, the catalytic combustion process is considered to be a promising technology. Catalytic combustion has many advantages over other technologies, such as thermal incineration and catalytic incineration in that they can efficiently decompose low concentrations of VOCs under mild conditions [3]. In addition, catalytic combustion leads to lower thermal NO_X emissions because the temperatures involved are relatively low [6].

Nowadays, CeO_2–ZrO_2 is one of the most important commercial catalytic support due to its use in the three-way catalysts [7]. It is applied in these systems owing to its high oxygen storage capacity. This material has been investigated since the early 1990s and is now generally known that the incorporation of zirconium into the ceria lattice creates a higher concentration of defects, thus, improving the O^{2-} mobility; such mobility would explain the outstanding ability to store and release oxygen [8]. It is well known that the materials possess (i) a large oxygen storage capacity (OSC) via a facile $Ce^{4+} \leftrightarrow Ce^{3+}$ redox process

* Corresponding author. Tel.: +86 28 85418451; fax: +86 28 85418451.
E-mail addresses: liuzhimin2648@sina.com (L. Zhi Min), zhongjunbo@sohu.com, scuzhong@sina.com (G. Mao Chu).

0304-3894/$ – see front matter © 2007 Elsevier B.V. All rights reserved.
doi:10.1016/j.jhazmat.2007.08.032

and (ii) an ability of promoting dispersion of noble metals [9,10].

Alifanti et al. [11] investigated the catalytic combustion of toluene on catalysts of $LaCoO_3$ loaded on $Ce_{1-x}Zr_xO_2$. Their results showed that T_{10} and T_{90} is about 568 and 653 K, respectively.

Scirè et al. [12] showed that the T_{10} and T_{90} of toluene on Au/CeO_2 catalysts are 513 and 573 K, respectively. Okumura et al. [13] investigated the catalytic combustion of toluene on Pd-based catalysts and their results indicated that toluene can be completely converted at about 590 K.

The above study shows that the decomposition of volatile organic compounds has been difficult because of the low catalytic activity. Therefore, it is crucial to enhance catalytic activity of catalysts. Various techniques have been developed for development and modification of the platinum supported on Ce–Zr–O solid solution catalysts [14]. However, to our knowledge, there are few reports on activity of platinum supported on Ce–Zr–O solid solution modified by Y and Mn.

In this report, results of optimization of the catalyst preparation and the bench scale tests of these catalysts of honeycomb-type are presented. The objective of this work is to investigate the effect of two metals doping into $Ce_{0.50}Zr_{0.50}O_2$ on catalytic activity of $Pt/\gamma\text{-}Al_2O_3/Ce_{0.45}Zr_{0.45}M_{0.10}O_X$ (M = Y, Mn) and $Pt/\gamma\text{-}Al_2O_3/Ce_{0.40}Zr_{0.40}Y_{0.10}Mn_{0.10}O_X$ monolithic catalysts toward the catalytic combustion of toluene as the simulated VOC.

2. Experimental

2.1. Catalyst preparation

$Ce_{0.50}Zr_{0.50}O_2$, $Ce_{0.45}Zr_{0.45}Y_{0.10}O_X$, $Ce_{0.45}Zr_{0.45}Mn_{0.10}O_X$ and $Ce_{0.40}Zr_{0.40}Y_{0.10}Mn_{0.10}O_X$ were prepared by coprecipitation method with $NH_3{*}H_2O$ and $(NH_4)_2CO_3$ mixed $Ce(NO_3)_3$, $ZrOCO_3$, $Mn(NO_3)_2$ and $Y(NO_3)_3$ aqueous solutions with a nominal composition. The precipitate was filtered, washed with distilled water until no pH change could be detected, then calcined in air at 873 K for 4 h in a muffle furnace. These samples $Ce_{0.50}Zr_{0.50}O_2$, $Ce_{0.45}Zr_{0.45}Y_{0.10}O_X$, $Ce_{0.45}Zr_{0.45}Mn_{0.10}O_X$ and $Ce_{0.40}Zr_{0.40}Y_{0.10}Mn_{0.10}O_X$ were labeled as CZ, CZY, CZM and CZYM, respectively.

$\gamma\text{-}Al_2O_3$ ($S_{BET} = 151.8\ m^2\ g^{-1}$) supported platinum catalyst was prepared by impregnation method with an aqueous solution of H_2PtCl_6 in excess of solution. The resulting powders were dried at 383 K for 2 h and annealed at 773 K for 2 h, thus forming $Pt/\gamma\text{-}Al_2O_3$ (A) with wt(Pt) = 0.5%. Pt was deposited on CZ, CZY, CZM and CZYM powders by immersion method using H_2PtCl_6 solution. The resulting powders were dried at 383 K for 2 h and calcined at 773 K for 2 h, thus forming Pt/CZ, Pt/CZY, Pt/CZM and Pt/CZYM (B) with wt(Pt) = 0.5%. The powders (A) and (B) were blended in mass ratios 1:1 and desired H_2O was added to make slurry. The slurry was then coated on a monolithic substrate with 400 cell/in.^{2}, then dried at 383 K for 2 h and calcined at 773 K for 3 h. The catalyst power content loaded on all monolithic catalysts was 140 mg/ml. The catalysts $Pt/\gamma\text{-}Al_2O_3$/CZ, $Pt/\gamma\text{-}Al_2O_3$/CZY, $Pt/\gamma\text{-}Al_2O_3$/CZM and $Pt/\gamma\text{-}Al_2O_3$/CZYM obtained were designated as C1, C2, C3 and C4, respectively.

2.2. Characterizations of OSMs and catalysts

Surface area analysis of catalysts was carried out by the Brunauer–Emmet Teller (BET) method using Autosorb-ZXF-05 (Xibei Chemical Institute, China). The samples were evacuated for 3 h at 623 K, and then cooled to 77 K using liquid N_2 at which point N_2 adsorption was measured. Oxygen storage capacity was determined by measuring oxygen storage amount in a conventional flow apparatus using TCD detector. All the samples (200 mg) were reduced in a quartz U-tube in H_2 stream at 823 K for 45 min, then cooled down to 473 K under pure N_2 stream. The samples remained at 473 K during the analysis. Then pulse of oxygen was injected up to the breakthrough point. OSC was evaluated from oxygen consumption.

X-ray diffraction (XRD) patterns were carried out on a DX-1000 X-ray diffractometer using Cu Kα ($\lambda = 0.15406$ nm) radiation equipped with a graphite monochromator. The X-ray tube was operated at 45 kV and 25 mA. Samples were scanned from 2θ equal to 10° up to 90° and the X-ray diffraction line positions were determined with a step size of 0.03° and a slit of 1.

Temperature-programmed reduction (H_2-TPR) experiments were carried out in a conventional system equipped with a thermal conductivity detector. All samples (100 mg) were pretreated in a quartz U-tube in a flow of pure N_2 at 673 K for 1 h, and then cooled down to room temperature. The reduction was carried out in a flow of H_2 (5%) in N_2 (20 ml min^{-1}) from 373 to 1073 K with a linear heating rate of 10 K min^{-1}.

Carbon monoxide chemisorption was used to determine the Pt dispersion of catalysts. Before the analyses, all the samples (500 mg) were reduced in a quartz U-tube in H_2 stream at 773 K for 60 min, and then cooled down to 313 K under pure N_2 stream. Then pulse of carbon monoxide was injected up to the breakthrough point. Dispersion of Pt was evaluated from the consumption of carbon monoxide (assuming CO/M = 1).

2.3. Activity measurement

The activity measurements were carried out in a conventional fixed-bed flow reactor. Schematic set-up of the equipment was shown in Fig. 1. Pressed air (oxygen pressure is around 0.1 MPa) was pumped into a three-neck bottle, which was immersed in ice-water bath; the three-neck bottle was filled with commercial toluene. The flask was sealed with inlet for pumped air and outlet for toluene vapor was brought by air. A thermometer was inserted under toluene surface to monitor the temperature of toluene. The desired flow-rate was maintained by a flowmeter. All gas lines of the apparatus are kept at 393 K in order to minimize VOC adsorption on the walls. The gaseous products were analyzed with an on-line gas chromatograph (GC-2000) using a Porapak T column, equipped with thermal conductivity detector (TCD) and a flame ionisation detector (FID).

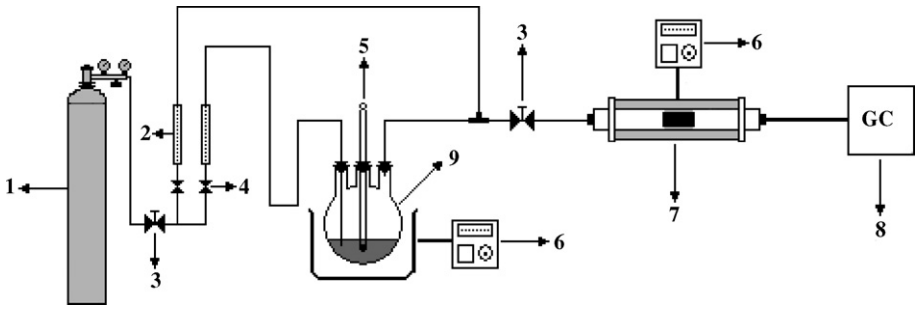

Fig. 1. Experimental set-up used for the catalytic combustion experiments (1) Air cylinder; (2) rotameters; (3) control valves; (4) switch valves; (5))thermometer; (6) temperature control system; (7) reactor; (8) gas chromatograph with an FID detector; (9) bubbling bottle containing saturated toluene.

3. Results and discussion

3.1. BET results and oxygen storage capacity of OSMs

The textural properties such as surface area play an important role in the performance of catalytic supports. Table 1 shows the textural properties and the oxygen storage capacity of the various OSMs. It is clear that the specific surface areas of these OSMs are all larger than 80 $m^2\,g^{-1}$ and in the order of CZY > CZYM > CZM > CZ. As shown in Table 1, after calcination at 873 K, the surface area of CZ is 87.68 $m^2\,g^{-1}$. Y^{3+} is incorporated into the $Ce_{0.50}Zr_{0.50}O_2$ solid solution lattices, resulting in the generation of $Ce_{0.45}Zr_{0.45}Y_{0.10}O_X$ solid solution; the surface area increases to 105.27 $m^2\,g^{-1}$. For CZM and CZYM, the surface area increases to 97.73 and 103.32 $m^2\,g^{-1}$, respectively.

The results of the oxygen storage capacity in Table 1 show that the OSC of CZY is very close to CZ. This indicates that doping Y^{3+} into $Ce_{0.50}Zr_{0.50}O_2$ has no obvious effect on OSC. Compared with the CZ and CZY, the OSC of CZM and CZYM are 763.8 and 596.7 μmol g^{-1}, respectively, which shows incorporation of Mn into the ceria–zirconia mixed oxides framework can greatly improve the capacity of storage. The results are consistent with the results of Ref. [15].

3.2. XRD characterization

X-ray diffraction was used to determine the bulk crystalline phases in the samples. The diffraction patterns of four types of OSMs are shown in Fig. 2. Four characteristic diffraction peaks are observed and indexed as cubic type crystallite. All the diffraction peaks for the product can be indexed to (1 1 1), (2 0 0), (2 2 0) and (3 1 1) crystal faces, corresponding to a face-centered cubic (fcc) fluorite structure of CeO_2 (JCPDs No. 34-0394). No separated CeO_2, ZrO_2, MnO_X and Y_2O_3 are detected by XRD

Table 1
The surface area and oxygen storage capacity of different OSMs

Sample	BET area ($m^2\,g^{-1}$)	OSC (μmol g^{-1})
CZ	87.68	464.2
CZY	105.27	445.3
CZM	97.73	763.8
CZYM	103.32	596.7

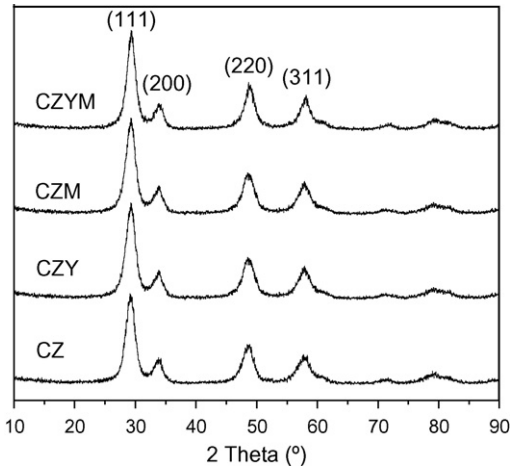

Fig. 2. XRD patterns of OSMs.

in the 2θ region from 10° to 90°, which indicates that Y, Mn, Y and Mn ions are doped into the ceria–zirconia mixed oxides framework forming the CeO_2–ZrO_2 mixed oxides. All these results clearly show that these supports are solid solution.

3.3. Temperature-programmed reduction

The H_2-TPR profiles of these OSMs are plotted in Fig. 3. The CZ mixed oxide has a broad peak centered at 911 K (Fig. 3, trace

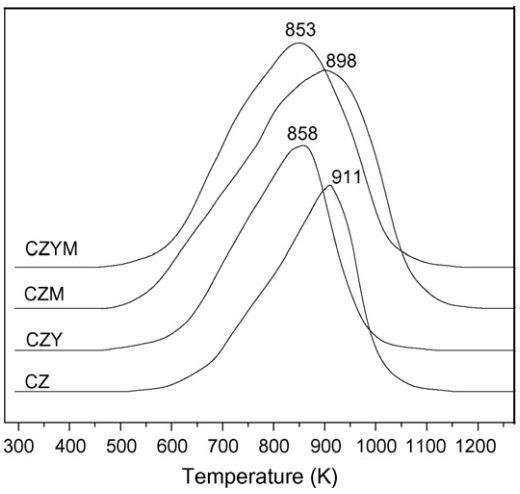

Fig. 3. H_2-TPR profiles of different OSMs.

CZ), which is attributed to the reduction of the Ce^{4+} in the CZ solid solution [16]. For all the samples, the shapes of the main peaks have no obvious difference. The temperatures of main peaks are 911 K for CZ, 858 K for CZY, 898 K for CZM and 853 K for CZYM, correspondingly (Fig. 3). Seen from Fig. 3, it is obvious that the temperature of peak for CZY is lowest. The peak temperature of CZY is 858 K, which is lower than that of CZ solid solution. This indicates the promotion of Ce^{4+} reduction can be related to a high mobility and diffusion of bulk O_2 due to the creation of a defective structure by introduction of Y into $Ce_{0.5}Zr_{0.5}O_2$ lattice [17]; also in this case detectable enhancement of Ce^{4+} reduction was observed when doping Mn into $Ce_{0.5}Zr_{0.5}O_2$ lattice.

As we know, the peak area has a direct correlation with the amount of reductive species. The bigger the area of peak, the more the reductive species and the stronger the reductive capability is. Compared with the CZ and CZY solid solution, CZM and CZYM solid solution have the bigger peak area, which demonstrates that Mn incorporating into $Ce_{0.5}Zr_{0.5}O_2$ lattice has a positive effect on reductive capability for $Ce_{0.5}Zr_{0.5}O_2$ solid solution [15]. This result is in good harmony with the results of OSC analysis.

3.4. Dispersion of Pt on different catalysts

Carbon monoxide chemisorption results showed the dispersion of Pt on C1, C2, C3 and C4 is about 47%, 50%, 51% and 53%, respectively. These results indicate that the dispersion of Pt has no obvious difference when doping Y, Mn, Y and Mn into $Ce_{0.50}Zr_{0.50}O_2$, simultaneously.

3.5. Catalytic performance

The results of blank experiment show the T_{10} of toluene over the four supports has no great difference. T_{10} of toluene over the four supports is around 570 K; the T_{90} of toluene over the four supports is around 700 K. So the catalytic activity of these supports is quite low.

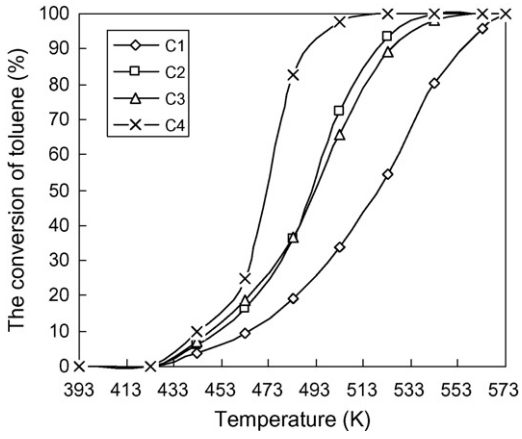

Fig. 4. Toluene conversion as a function of reaction temperature on catalysts (GHSV = 12000 h^{-1}).

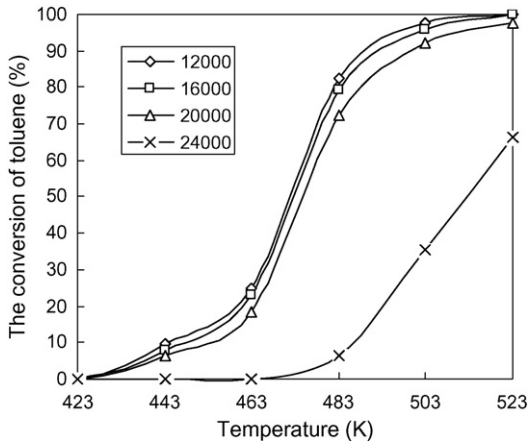

Fig. 5. Effect of GHSV for toluene conversion on $Pt/Al_2O_3/Ce_{0.40}Zr_{0.40}Y_{0.10}Mn_{0.10}O_x$.

Fig. 4 shows the light-off curve of toluene (500 ppm in air) on different catalysts. Experiments were done under a space velocity 12,000 h^{-1}. Under the investigated conditions, CO_2 and water are the only reaction products detected. As show in Fig. 4, the conversion of toluene increases with the increasing of reaction temperature. However, the extent of increase in activity differs considerably from catalyst to catalyst under same conditions. The activity of the four catalysts is of the order C4 > C3 ≈ C2 > C1. The T_{10} of toluene on C1, C2, C3, and C4 is 464, 453, 449 and 443 K, respectively; the corresponding complete conversion temperature of toluene is 555, 519, 524 and 489 K, respectively. The results indicate that doping Y, Mn, Y and Mn into $Ce_{0.50}Zr_{0.50}O_2$ can promote the activity of the catalyst. When doping Y and Mn into ceria–zirconia mixed oxides simultaneously, Pt/Al_2O_3/CZYM shows the highest activity for toluene catalytic combustion.

Based on these experiments, we selected optimum composition and supporting conditions to obtain sample of the highest activity. So, sample C4 was chosen to investigate the effect of GHSV on the catalytic activity. The results were present in Fig. 5.

As shown in Fig. 5, the activity of the catalyst does not decrease as much with the increase of GHSV in the range of 12,000–20,000 h^{-1}; when the GHSV is beyond 20,000 h^{-1}, the activity of the catalyst decreases dramatically. When the GHSV is 24000 h^{-1}, the light-off temperature of the toluene increases to 673 K. As to the negative effect of higher GHSV, it can be speculated to be caused by the following factors. On one hand, the reaction of toluene combustion is exothermic reaction, much more heat was carried off as the increasing of GHSV; on the other hand, increasing of GHSV shortens the time of the contact of the reactant with the catalyst. When GHSV is low, the catalysts give more favorable results. So, it is obvious that the prepared catalyst can be applied in a wide range of GHSV operations.

4. Conclusions

The paper revealed that the catalytic activity of $Pt/Al_2O_3/Ce_{0.50}Zr_{0.50}O_2$ for toluene combustion can be greatly improved

by doping Y, Mn, Y and Mn into $Ce_{0.50}Zr_{0.50}O_2$. The characterization results of XRD indicate doping Y, Mn, Y and Mn into $Ce_{0.50}Zr_{0.50}O_2$ can form CeO_2–ZrO_2 solid solution. Doping Mn into $Ce_{0.50}Zr_{0.50}O_2$ can greatly improve the capacity of storage. Temperature-programmed reduction results demonstrate that doping Y into $Ce_{0.50}Zr_{0.50}O_2$ has a positive effect on high mobility and diffusion of bulk O_2. When doping Y and Mn into $Ce_{0.50}Zr_{0.50}O_2$ simultaneously, the catalyst Pt/γ-Al_2O_3/$Ce_{0.40}Zr_{0.40}Y_{0.10}Mn_{0.10}O_X$ shows the highest activity. The T_{10} and T_{90} of toluene are 443 and 489 K, respectively. The GHSV results show that the prepared catalysts can be used in a wide range of GHSV.

References

[1] H.G. Lintz, K. Wittstock, The oxidation of solvents in air on oxidic catalysts—formation of intermediates and reaction network, Appl. Catal. A 216 (2001) 217–225.

[2] S.C. Kim, The catalytic oxidation of aromatic hydrocarbons over supported metal oxide, J. Hazard. Mater. B 91 (2002) 285–299.

[3] M. Alifanti, M. Florea, S. Somacescu, V.I. Parvulescu, Supported perovskites for total oxidation of toluene, Appl. Catal. B Environ. 60 (2005) 33–39.

[4] E. Dıaz, S. Ordonez, A. Vega, J. Coca, Evaluation of different zeolites in their parent and protonated forms for the catalytic combustion of hexane and benzene, Micro. Meso. Mater. 83 (2005) 292–300.

[5] M.W. Ryoo, S.G. Chung, J.H. Kim, Y.S. Song, G. Seo, The effect of mass transfer on the catalytic combustion of benzene and methane over palladium catalysts supported on porous materials, Catal. Today 83 (2003) 131–139.

[6] K.M. Parida, S. Amarendra, Catalytic combustion of volatile organic compounds on Indian Ocean manganese nodules, Appl. Catal. A Gen. 182 (1999) 249–256.

[7] P. Fornasiero, R.D. Monte, G. Rao, J. Kaspar, S. Meriani, A. Trovarelli, J. Graziani, Rh-Loaded CeO_2–ZrO_2 solid solutions as highly efficient oxygen exchangers: dependence of the reduction behavior and the oxygen storage capacity on the structural properties, J. Catal. 151 (1995) 168–177.

[8] Y.N. Asutaka, T. Yamamoto, T. Tanaka, X-ray absorption fine structure analysis of local structure of CeO_2–ZrO_2 mixed oxides with the same composition ratio (Ce/Zr = 1), Catal. Today 74 (2002) 225–237.

[9] H. He, H.X. Dai, K.W. Wong, C.T. Au, $RE_{0.6}Zr_{0.4-x}Y_xO_2$ (RE = Ce, Pr; x = 0, 0.05) solid solutions: an investigation on defective structure, oxygen mobility, oxygen storage capacity, and redox properties, Appl. Catal. A Gen. 251 (2003) 61–74.

[10] H. He, H.X. Dai, C.T. Au, Defective structure, oxygen mobility, oxygen storage capacity, and redox properties of RE-based (RE = Ce, Pr) solid solutions, Catal. Today 90 (2004) 245–254.

[11] M. Alifanti, M. Florea, V.I. Parvulescu, Ceria-based oxides as supports for LaCoO3 perovskite catalysts for total oxidation of VOC, Appl. Catal. B Environ. 70 (2007) 400–405.

[12] S. Scirè, S. Minicò, C. Crisafulli, Catalytic combustion of volatile organic compounds on gold/cerium oxide catalysts, Appl. Catal. B Environ. 40 (2003) 43–49.

[13] K. Okumura, T. Kobayashi, H. Tanaka, M. Niwa, Toluene combustion over palladium supported on various metal oxide supports, Appl. Catal. B Environ. 44 (2003) 325–331.

[14] F.J. Hodar, C.M. Castilla, A.F. Cadenas, Catalytic combustion of toluene on platinum-containing monolithic carbon aerogels, Appl. Catal. B Environ. 54 (2004) 217–224.

[15] A.E. Nelson, K.H. Schulz, Surface chemistry and microstructural analysis of $Ce_xZr_{1-x}O_{2-y}$ model catalyst surfaces, Appl. Surf. Sci. 210 (2003) 206–221.

[16] D. Terribile, A. Trovarelli, C. Leitenburg, A. Primavera, G. Dolcetti, Catalytic combustion of hydrocarbons with Mn and Cu-doped ceria–zirconia solid solutions, Catal. Today 47 (1999) 133–140.

[17] K. Minami, T. Masui, N. Imanak, L. Dai, B. Pacaud, Redox behavior of CeO_2–ZrO_2–Bi_2O_3 and CeO_2–ZrO_2–Y_2O_3 solid solutions at moderate temperatures, J. Alloy Comp. 408–412 (2006) 1132–1135.